A MEMS Phased Array Transducer for Ultrasonic Flaw Detection

A. Jain
Dept. Electrical and Computer Engineering
Carnegie Mellon University
Pittsburgh, PA, USA
akash@andrew.cmu.edu

D.W. Greve
Dept. Electrical and Computer Engineering
Carnegie Mellon University
Pittsburgh, PA, USA
dg07@andrew.cmu.edu

I.J. Oppenheim
Dept. Civil and Environmental Engineering
Carnegie Mellon University
Pittsburgh, PA, USA
ijo@andrew.cmu.edu

Abstract

Metal structures can fail because of fatigue crack propagation or because of section loss from corrosion. Regular inspection is required to detect such failures. We report here progress toward the development of MEMS-based transducers for ultrasonic flaw detection, to be permanently mounted at critical locations on structures. In a complete system, a single piezoelectric element will be used to emit a pulse of ultrasonic energy and an array of MEMS detectors will be used to detect echoes from nearby surfaces or flaws. In this paper, we report initial characterization of MEMS ultrasonic transducers, coupling of these transducers to a solid structure, and the use of multiple transducers to detect the distance and angular location of an ultrasonic source.

Keywords

ultrasonic MEMS transducer phased array

INTRODUCTION

MEMS diaphragm capacitive transducers (sometimes termed MUTs, for Micromachined ultrasonic transducers) have been studied by several groups. In prior work, these transducers have been coupled to gases or liquids [1,2,3,4] and have been applied for imaging [5,6] and non-destructive testing [7]. We are adapting capacitive diaphragm transducers for application to structural monitoring. In this application we intend to permanently couple the transducers to a solid structure. We propose to use a single piezoelectric transducer as a source of ultrasonic energy, while an array of capacitive transducers is to be used as the detectors. In this way we can take advantage of the high efficiency of piezoelectric emitters when coupled to solids with similar acoustic impedance. The array of MEMS detectors will be used as a phased array in order to scan for defects or cracks near the emitter.

In this paper, we report recent results on several aspects of this development. First, we report a method for direct coupling of the detector to a solid. We then illustrate the use of a detector array to detect the direction and angular location of an ultrasonic source.

DEVICE DESIGN, FABRICATION AND BONDING

Figure 1 shows the top view and cross section of one capacitive diaphragm. The structure shown was fabricated in the multi-user MUMPS process and was designed for a resonant frequency near 5 MHz. The gap between electrodes is 2.0 microns and the thickness of the upper polysilicon electrode is also 2.0 microns. Holes approximately 5 microns square are placed approximately 30 microns apart to provide for etching and release of the diaphragm. Devices were released at CRONOS using wet etching followed by supercritical drying. Subsequently back contacts were provided by etching the back surface of the wafer with concentrated HF followed by deposition of aluminum. This structure is somewhat non-optimal in that the parasitic capacitances to ground are rather large. In addition, the design does not take advantage of the DIMPLE mask to reduce the spacing between the diaphragm electrodes.

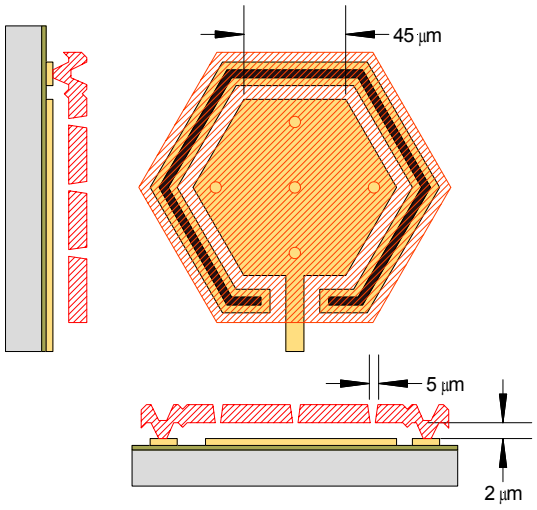

Figure 1. Single diaphragm unit

A CAD drawing showing the complete chip is shown in Figure 2. Detectors consisted of 180 individual diaphragms connected in parallel. The detector array investigated here is at the right edge of the drawing; other structures on the chip had different geometry and are not discussed here.

consisted of nine individual detectors with centers spaced 0.99 mm apart. .

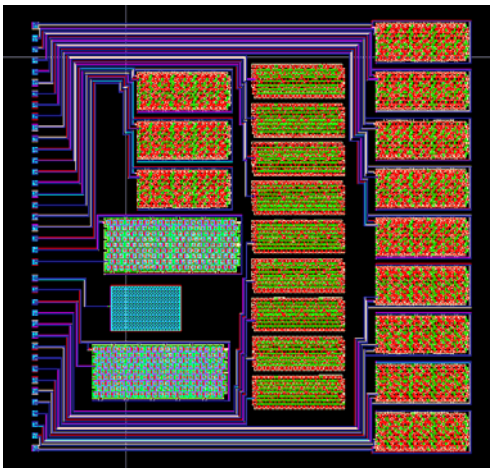

Figure 2. Chip layout.

Experiments reported here were performed using prism-shaped plexiglas test specimens (Figure 3). Released chips were bonded to the plexiglas using Gelest Zipcone silicone coating, which was brush-applied followed by chip placement. In earllier work, we have attached chips to aluminum test specimens using cyanoacrylate adhesive [8]. This was only partially successful in that only a few detectors were undamaged. With the silicone coating eight out of nine detectors were working after chip placement. It was possible to image the chip surface through the plexiglas and only a few small (~ 50 μm diameter) bubbles were observed, covering less than 5% of the total detector area. The transducers were contacted using a standard probe station.

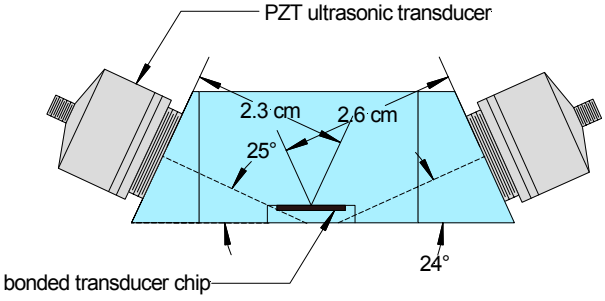

Figure 3. Plexiglas specimen used for testing of the ultrasonic transducer arrays.

TRANSDUCER CHARACTERIZATION

Capacitance-voltage measurements were performed prior to ultrasonic testing in order to verify transducer operation. Figure 4 shows 1 MHz capacitance-voltage measurements [9] on two bonded transducers. The plotted data for the two transducers are offset vertically for clarity. Data obtained for an *unbonded* transducer is shown as a black dashed line for comparison.

For the unbonded transducer the data closely follows the expected relationship

$$C(V) = C_0 + C_1 V^2$$

and no hysteresis is observed. The value of C_1 can be predicted with good accuracy using a single-degree-of-freedom model for the diaphragm [10]. In contrast, the measurements on bonded transducers shows significant hysteresis and less change in capacitance with applied voltage. We conclude that the bonded transducers deflect less than unbonded transducers because they are attached to the plexiglas wedge. The hysteresis is attributed to "flow" of the silicone coating. Very similar C(V) measurements were obtained for several bonded transducers on the same chip, indicating that the transducers were mechanically and electrically nearly identical.

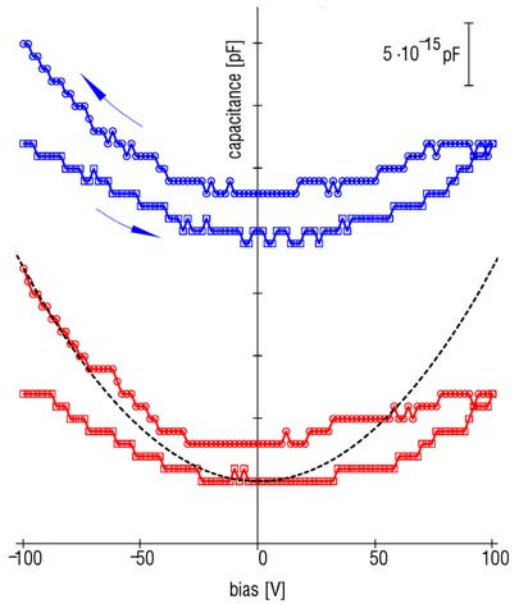

Figure 4. 1 MHz capacitance-voltage measurements for two bonded transducers (points) and for unbonded transducer (dashed line).

Ultrasonic detection experiments utilized a Krautkramer USPC-2100 to drive a 5 MHz Krautkramer MSW-QC transducer with short pulses. Individual diaphragm detectors were biased with up to 100 V DC and the detected signal was recorded using a HP 54601A oscilloscope. Figure 5 illustrates the measurement circuit. It is important to note that the magnitude of the observed signal is substantially reduced by stray capacitance associated with parasitics in our detector design, cable capacitance, and oscilloscope input capacitance. We will discuss later changes which will lead to increased signal strengths. Nevertheless, signals are detectable with this arrangement and are strong enough to demonstrate detector operation.

The oscilloscope was triggered by the incident ultrasonic pulse in order to provide a known time origin. Signals collected by the oscilloscope were averaged over multiple

pulses, transferred to a PC running Labview, and stored to a file for later analysis. Due to probing limitations, only one signal was collected at a time; multiple signals from the phased array were combined during off-line analysis.

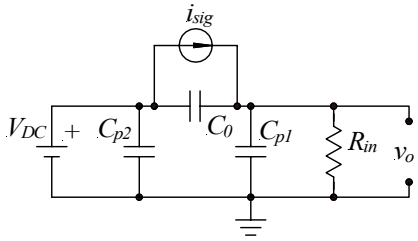

Figure 5. Test circuit.

In a capacitive transducer the signal current is given by

$$i_{sig} = C_0 \frac{dv}{dt} + v\frac{dC}{dt} \approx V_{DC}\frac{\varepsilon_0 S^*}{g^2}\frac{dx}{dt}$$

where *dx/dt* is the velocity of the top plate of the diaphragm, V_{DC} the DC bias voltage, S^* the detector effective area, and g isthe gap between top and bottom electrodes. Figure 6 illustrates the observed signals as a function of DC bias voltage on the detectors for an ultrasonic pulse uniformly incident on all detectors (transmitter 1.35 cm from the detector chip, not shown in Figure 3). The emitted pulse is at t = 1 μs and is visible due to stray electrical coupling even with zero DC bias. A received pulse appears only when a DC bias is applied and is approximately linearly dependent on the DC bias as expected. The received pulse occurs approximately 4.9 μs after the emitted pulse, which is in good agreement with the delay of 5.0 μs predicted using the velocity of sound in plexiglas (c = 2700 m/sec). (The bottom trace shows the result of a point-by-point subtraction of the signals with V_{DC} = 0 V and V_{DC} = 100 V. This confirms that the signal at t = 1 μs is due to electrical coupling.)

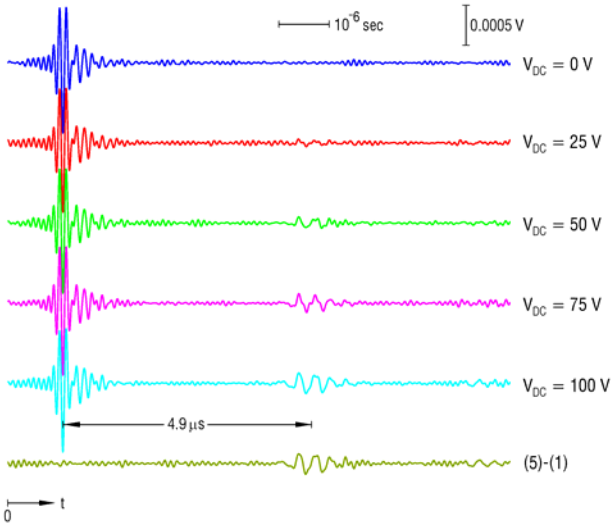

Figure 6. Received pulses for normal incidence (source 1.35 cm fromdetectors).

We now consider the use of the ultrasonic detector array to detect off-axis signals. Figure 7 shows the results obtained for a transducer in position #1 in Figure 3. Transducers are numbered beginning with the left hand edge so the transducer nearest to this source is #1 and the most distant is #9. As expected, we observe increasing delay moving from #1 to #9. (Transducer #4 was initially non-functional and transduer #8 failed or was damaged in the course of measurements). The delay between transducers is given by

$$\Delta t = \frac{d\cos(\theta)}{c}$$

where d is the spacing between transducers and θ is the angle between the emitting transducer and the chip surface (θ = 25 degrees for emitter location #1).

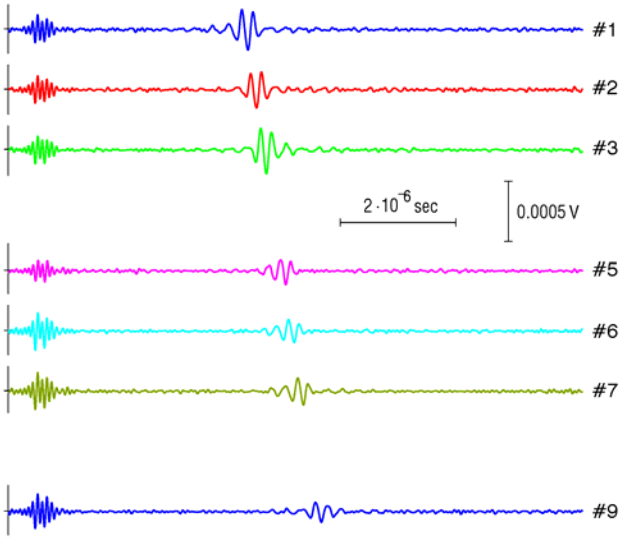

Figure 7. Received pulses with source at location #1.

Figure 8 illustrates the determination of the delay time between transducers. We plot a sum of delayed signals given by

$$V(t,\tau) = \sum_n v_n(t - n\cdot\tau)$$

where $v_n(t)$ is the signal from the nth transducer and τ is the delay. This results in a summed signal which depends on the delay time τ. These summed signals are plotted in Figure 8. We observe that all transducer signals add coherently to give the largest summed signal for τ = 330 ns. This yields θ = 29 degrees, in reasonable agreement with the prism shape. The total delay of the pulse corresponding to the transducer #5 (the center transducer) is approximately 9.7 μs. This gives a distance to the source of 2.35 cm, in excellent agreement with the prism shape.

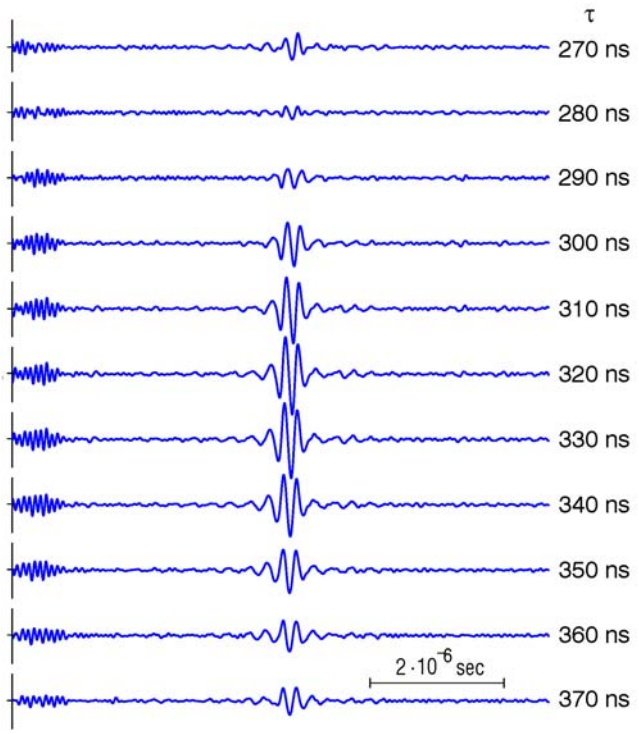

Figure 8. Sum of delayed signals as a function of the delay time τ. A maximum amplitude is obtained when all signals add coherently at τ = 330 ns.

Localization of a source by phased-array detection can be illustrated more vividly by making a contour plot of $|V(t,\tau)|$. On this contour plot the angular position of a source is related to the peak position on the τ axis while the distance is proportional to the peak location on the t axis. Figure 9 shows these contour plots for the two detector locations indicated in Figure 3. Note that times should be measured with respect to the origin determined by the source delay at (t = 2 μsec, τ = 0). The data clearly show that detector #1 is more distant from the leftmost detector than detector #2, and that τ is negative for the second detector as expected.

CONCLUSIONS

We report here for the first time the application of MEMS capacitive diaphragm transducers directly coupled to solids. These transducers can potentially be applied to structural monitoring. We have also demonstrated phased-array detection of the location and angular position of a source, which will be necessary when detectors are permanently fixed.

The signal levels reported in this work are small (~mV). There are a number of changes which can be made to substantially improve these signal levels, however. Even within the context of the MUMPS process, transducer sensitivity can be increased by using the DIMPLE mask to reduce the gap from 2.0 mm to about 1.4 mm. More significant improvements will result from redesigning the diaphragm supports to reduce the parasitic capacitance to ground. Transducers with improved design are presently being fabricated in MUMPS and will be reported on in a future publication.

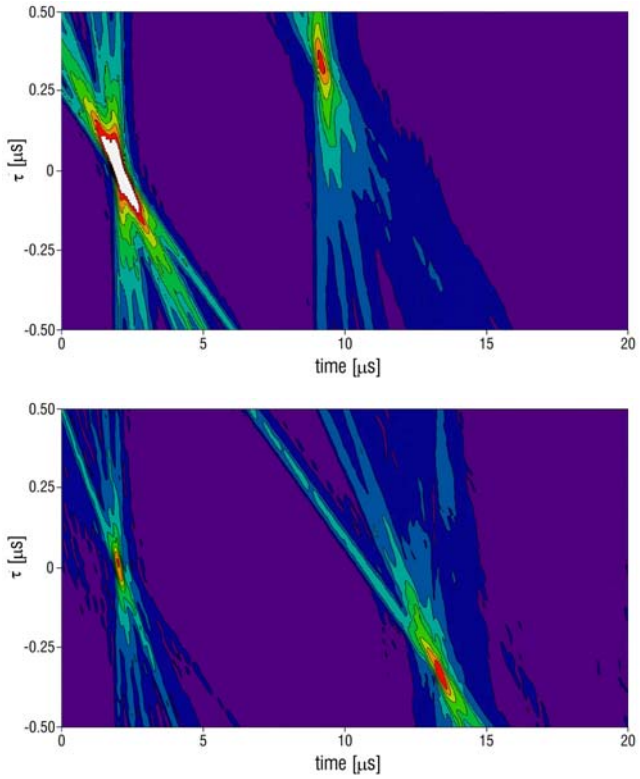

Figure 9. Contour plots of $|V(t,\tau)|$: (top) source at location #1, and (bottom) source at location #2.

ACKNOWLEDGEMENTS

This work has been funded by the Commonwealth of Pennsylvania through the Pennsylvania Infrastructure Technology Alliance program, administered at Carnegie Mellon by the Institute for Complex Engineering Systems, and by gifts from Krautkramer Inc., and the authors gratefully acknowledge that support.

REFERENCES

[1] "Surface micromachined ultrasound transducers in CMOS technology," P.-C. Eccardt, K. Niederer, T. Scheiter, and C. Hierold, 1996 IEEE Ultrasonics Symposium, pp. 959-962 (1996).

[2] "Micromachined ultrasonic capacitance transducers for immersion applications," A.G. Bashford, D.W. Schindel, D.A. Hutchins, IEEE Transactions on Ultrasonics, Ferroelectrics, and Frequency Control, vol. 45, pp. 367-375 (1998).

[3] "Characterization of one-dimensional capacitive micromachined ultrasonic immersion transducer arrays," X. Jin, I. Ladabaum, F.L. Degertekin, S. Calmes, and B.T. Khuri-Yakub, IEEE Journal of Microelectromechanical Systems, vol. 8, pp. 100-114 (1999).

[4] "Characterization of one-dimensional capacitive micromachined ultrasonic immersion transducer arrays," X. Jin, O. Oralkan, F.L. Degertekin, and B.T. Khuri-Yakub, IEEE Transactions on Ultrasonics, Ferroelectrics, and Frequency Control, vol. 48, pp. 750-760 (2001).

[5] "Initial pulse-echo imaging results with one-dimensional capacitive micromachiined ultrasonic transducer arrays," O. Oralkan, X.C. Jin, K. Kaviani, A.S. Ergun, F.L.Degertekin, M. Karaman, and B.T. Khuri-Yakub, 2000 IEEE Ultrasonics Symposium, pp. 959-962 (2000).

[6] "Micromachined transducers for ultrasound applications," P.-C. Eccardt, K. Niederer, and B. Fischer, 1997 IEEE Ultrasonics Symposium, pp. 1609-1618 (1997).

[7] "Air-coupled nondestructive evaluation using micromachined ultrasonic transducers," S.T. Hansen, B.J. Mossawir, A.S. Ergun, F. L. Degertekin, and B.T. Khuri-Yakub, 1999 IEEE Ultrasonics Symposium, pp. 1037-1040 (1999).

[8] "A MEMS Ultrasonic Transducer for Monitoring of Steel Structures," A. Jain, D.W. Greve, and I.J. Oppenheim (to appear in SPIE Proceedings, Spring, 2001).

[9] 1 MHz is far from the resonant frequency of the unbonded diaphragms and consequently these measurements can be used to observe the deflection of the diaphragm by an applied DC voltage.

[10] I.J. Oppenheim, A. Jain, and D.W. Greve, (in preparation).

[1] "Surface micromachined ultrasound transducers in CMOS technology," P.-C. Eccardt, K. Niederer, T. Scheiter, and C. Hierold, 1996 IEEE Ultrasonics Symposium, pp. 959-962 (1996).
[2] "Micromachined ultrasonic capacitance transducers for immersion applications," A.G. Bashford, D.W. Schindel, D.A. Hutchins, IEEE Transactions on Ultrasonics, Ferroelectrics, and Frequency Control, vol. 45, pp. 367-375 (1998).
[3] "Characterization of one-dimensional capacitive micromachined ultrasonic immersion transducer arrays," X. Jin, I. Ladabaum, F.L. Degertekin, S. Calmes, and B.T. Khuri-Yakub, IEEE Journal of Microelectromechanical Systems, vol. 8, pp. 100-114 (1999).
[4] TITLE X. Jin, O. Oralkan, F.L. Degertekin, and B.T. Khuri-Yakub, IEEE Transactions on Ultrasonics, Ferroelectrics, and Frequency Control, vol. 48, pp. 750-760 (2001).
[5] "Initial pulse-echo imaging results with one-dimensional capacitive micromachiined ultrasonic transducer arrays," O. Oralkan, X.C. Jin, K. Kaviani, A.S. Ergun, F.L.Degertekin, M. Karaman, and B.T. Khuri-Yakub, 2000 IEEE Ultrasonics Symposium, pp. 959-962 (2000).
[6] "Micromachined transducers for ultrasound applications," P.-C. Eccardt, K. Niederer, and B. Fischer, 1997 IEEE Ultrasonics Symposium, pp. 1609-1618 (1997).
[7] "Air-coupled nondestructive evaluation using micromachined ultrasonic transducers," S.T. Hansen, B.J. Mossawir, A.S. Ergun, F. L. Degertekin, and B.T. Khuri-Yakub, 1999 IEEE Ultrasonics Symposium, pp. 1037-1040 (1999).
[8] our SPIE paper reference
[9] 1 MHz is far from the resonant frequency of the unbonded diaphragms and consequently these measurements can be used to observe the deflection of the diaphragm by an applied DC voltage.
[10] I.J. Oppenheim, A. Jain, and D.W. Greve, (in preparation).